Analog Integrated Circuits and Signal Processing, 12, 239–253 (1997)

Interaction of Capacitive and Resistive Nonlinearities in Chua's Circuit

ALI OKSASOGLU[1] **AND LAWRENCE P. HUELSMAN**

Department of Electrical & Computer Engineering, University of Arizona, Tucson, AZ 85721

Received February 29, 1996; Accepted October 11, 1996

Abstract. The interaction of capacitive and resistive nonlinearities in the Chua's circuit is studied. The original Chua's circuit is modified by replacing one of the linear capacitors with a nonlinear one to investigate the effects of such an interaction on the chaotic behavior of the circuit. It is found that such an interaction can be effective in limiting and controlling chaos. The Pspice simulation results are also given and compared with our numerical solutions.

Key Words: Chua's circuit, chaos

1. Introduction

The chaotic nature and the behavior of the Chua's circuit whose only nonlinear element is a three-segment piecewise linear resistor has already been repeatedly studied (e.g., see [1]–[3]). This nonlinear resistor, also called the Chua's diode, is available as an IC chip [4], or can easily be realized by using two op amps and six linear resistors [5]. The fact that this circuit is very simple, easy to implement, and rich in behavior has made it very popular for analytical and experimental investigation of chaos. In this paper, we numerically investigate the interaction of capacitive and resistive nonlinearities in the Chua's circuit, and discuss the effects of such an interaction on the chaotic behavior of the circuit. Our numerical results are verified by the Pspice (e.g., see [6]) simulations. For this purpose, the original Chua's circuit is modified by replacing one of the linear capacitors in the circuit with a nonlinear one whose nonlinearity is represented by a third-order polynomial. Such polynomial representations are often used in the study of certain nonlinear systems (e.g., see [7]–[10]). The circuit realization is shown in Fig. 1. In the rest of the paper, we will refer to the Chua's circuit as the original, and to the circuit of Fig. 1 as the modified. By appropriate choice of parameters, the modified circuit can be used to study the effects of the resistive and capacitive nonlinearities individually, or both nonlinearities together. Thus, in that sense, the modified circuit can be viewed as a generalization of the original circuit. A similar study was conducted in [10] for a second-order nonautonomous RL-varactor diode circuit. To simulate the chaotic behavior from this circuit, the varactor diode was modeled as a parallel combination of a nonlinear capacitor and a nonlinear resistor. It was shown that such an interaction of the capacitive and the resistive nonlinearity can be a promising way of limiting chaos.

2. Analysis

In the circuit, the interaction of resistive and reactive nonlinearities in general can be studied by making one or all the reactive elements nonlinear. However, the most interesting results are observed in the case of the capacitor C_2 being nonlinear as opposed to the case of the capacitor C or the inductor L being nonlinear. Therefore, for brevity, we will confine our discussion only to the case of the capacitor C_2 being nonlinear. For the purpose stated above, let us assume that the nonlinear capacitor C_2 in Fig. 1 is a charge-controlled one, and that its $v-q$ characteristic is given by $v_2(t) = f(q_2) = a_1 q_2 + a_3 q_2^3$. The governing equations for the voltage v_1 across the linear capacitor C, the current i_L through the inductor L, and the charge q_2 of the nonlinear capacitor are given by the following set of three first-order nonautonomous differential equations:

$$\begin{aligned} \frac{dq_2}{dt} &= G[v_1 - f(q_2)] - h(f(q_2)) \\ \frac{dv_1}{dt} &= \frac{1}{C} i_L - \frac{G}{C}[v_1 - f(q_2)] \end{aligned} \tag{1}$$

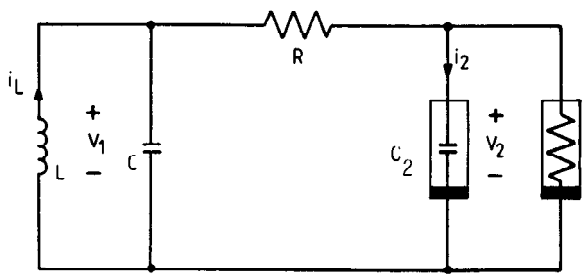

Fig. 1. Modified circuit realization.

$$\frac{di_L}{dt} = -\frac{1}{L}v_1$$

where $h(\cdot) = G_1(\cdot) + 0.5(G_0 - G_1)(|(\cdot) + B_p| - |(\cdot) - B_p|)$ is a three-segment piecewise linear function for the Chua's diode with G_0, G_1 as the slope, and B_p the break point for those segments. For such systems, it is usually more convenient to work with nondimensional variables and parameters. Hence, we use the following change of variables for that purpose:

$$\begin{aligned} \tau &= \omega_0 t \\ q_2 &= q_0 x \\ v_1 &= V_0 y \\ i_L &= I_0 z \end{aligned} \tag{2}$$

where ω_0, q_0, V_0, and I_0 are any arbitrary positive frequency, charge, voltage, and current scaling factors, respectively. Here, x, y, and z are the new respective nondimensional charge, voltage, and the current variables. By substituting (2) in (1), we obtain the following nondimensional set of differential equations:

$$\begin{aligned} \frac{dx}{d\tau} &= \alpha[y - r(g(x))] \\ \frac{dy}{d\tau} &= \gamma[g(x) - y + \eta z] \\ \frac{dz}{d\tau} &= -\beta y \end{aligned} \tag{3}$$

where $g(x) = ax + bx^3$, and $r(\cdot) = m_1(\cdot) + 0.5(m_0 - m_1)(|(\cdot) + \varepsilon| - |(\cdot) - \varepsilon|)$ with

$$\begin{aligned} a &= \frac{a_1 q_0}{V_0} \\ b &= \frac{a_3 q_0^3}{V_0} \end{aligned}$$

$$\begin{aligned} m_0 &= 1 + \frac{G_0}{G} \\ m_1 &= 1 + \frac{G_1}{G} \\ \varepsilon &= \frac{B_p}{V_0} \end{aligned} \tag{4}$$

The other nondimensional parameters in (3) are given as

$$\begin{aligned} \alpha &= \frac{GV_0}{q_0\omega_0} \\ \beta &= \frac{V_0}{I_0\omega_0 L} \\ \gamma &= \frac{G}{C\omega_0} \\ \eta &= \frac{I_0}{GV_0} \end{aligned} \tag{5}$$

Note that with the choice of $(\gamma, a, b, \eta, \varepsilon) = (1, 1, 0, 1, 1)$ the system of (3) represents the original circuit. On the other hand, the choice of $(m_1, \varepsilon) = (1, 0)$ leaves only the capacitive nonlinearity in the circuit. Since the objective of the paper is to investigate the interaction of different types of nonlinearity, the case of only the capacitive nonlinearity is not discussed here. For illustration purposes, in Fig. 2 we give a chaotic attractor from the modified circuit projected onto the $x - y$ plane. This attractor is obtained by choosing $(\alpha, \varepsilon, a, b) = (6.4, -0.2, -1.4, 0.98)$. We see that there is a structural difference between the double-scroll attractor [3] from the original circuit, and the attractor of Fig. 2. In the simulations, where not specified otherwise, we use $(\alpha, \beta, \gamma, m_0, m_1, \varepsilon, \eta) = (9, 100/7, 1, -1/7, 2/7, 1, 1)$ as in the case of the original circuit.

3. Effects of the Interaction

In this section, we present a two-dimensional bifurcation diagram to show the effects of the interaction of the resistive and the capacitive nonlinearities in the circuit. This bifurcation diagram in the $m_0 - m_1$ plane for three different values of b, namely, 0.0, -0.01, and -0.02, is given in Fig. 3. Note that since b is the coefficient of the cubic nonlinearity for the nonlinear capacitor, the case of $b = 0$ corresponds to the original circuit. For the consistency of our comparisons, we keep the values of the other parameters same as those of the

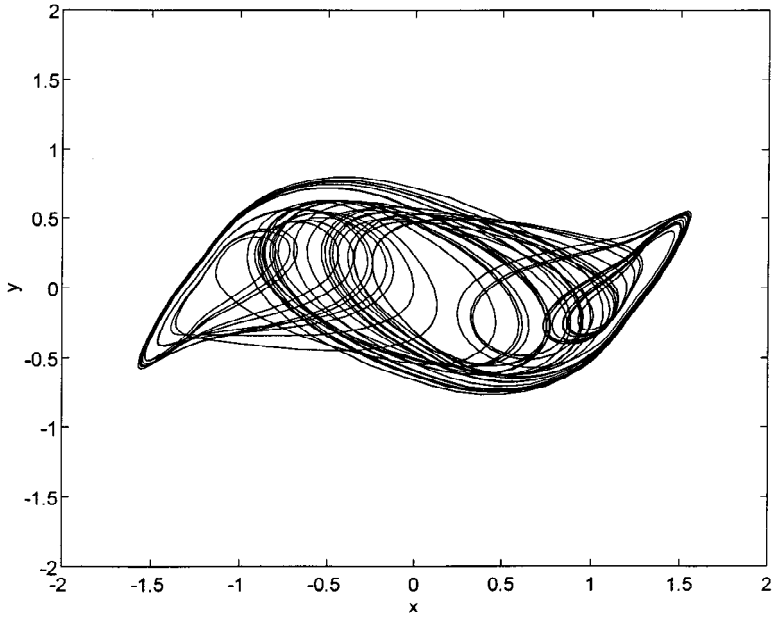

Fig. 2. A chaotic attractor from the modified circuit.

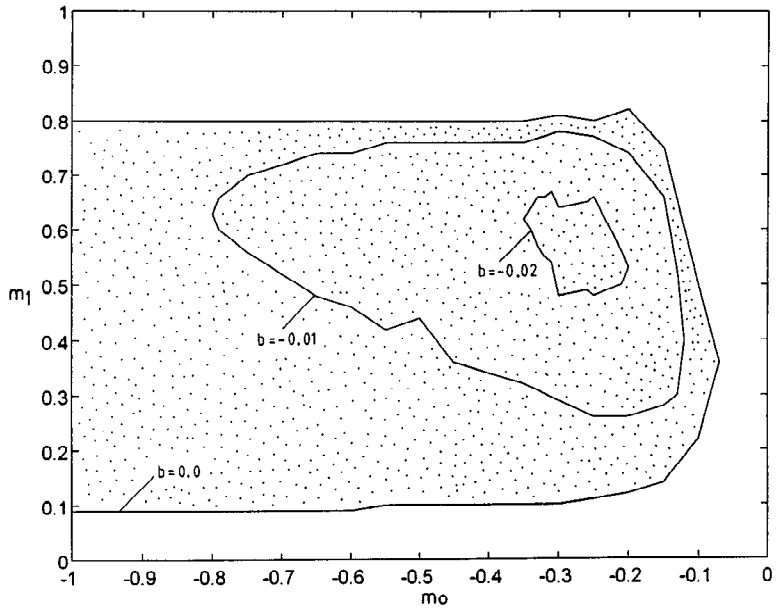

Fig. 3. Two-parameter bifurcation diagram in the $m_0 - m_1$ plane.

original circuit. The dotted areas in this diagram show the chaotic regions, and the darker lines represent the outer boundaries for the respective chaotic regions for different values of b. From this figure, we see that the region of chaos is the largest when $b = 0$, i.e., when no capacitive nonlinearity exists. However, as b increases in magnitude, the chaotic motion is confined to a smaller region in the parameter space. Thus, we can say that the addition of the capacitive nonlinearity in this case plays a limiting role on chaos. Although each chaotic region in Fig. 3 has some small windows of order, the qualitative behavior of the system is not affected by them. The routine used to integrate the system of (3) is a fourth-order Runge-Kutta algorithm with a stepsize less than 0.01.

4. Spice Simulations

In this section, we use SPICE to simulate the circuit of Fig. 1 to verify the bifurcation diagram of Fig. 3. The most important steps in the simulations will be the realization of the Chua's diode, and the charge-controlled nonlinear capacitor. A realization of Chua's diode using two op amps and six linear resistors is given in [11]. Thus, for that part of the circuit, we will use the same method outlined in [11] for different values of m_0, and m_1. As for the simulation of a charge-controlled nonlinear capacitor whose $v - q$ characteristic is given by $v(q) = \sum_k a_k q^k$, we can employ the circuit shown in Fig. 4. In this circuit, the dependencies of the dependent sources are given as

$$v_1 = v_0, \qquad i_x = i, \qquad i_0 = \sum_k b_k v_x^k \quad (6)$$

By using (6), we can express the port voltage $v(t)$ of Fig. 4 as a function of $q(t)$, where $q(t) = \int_\tau i(\tau)d\tau$, as

$$v(t) = \sum_k R_x b_k \frac{q^k}{C_x^k} \quad (7)$$

Thus, the relationship between the actual circuit parameters a_k, and the simulation parameters b_k can be given as

$$b_k = \frac{C_x^k}{R_x} a_k \qquad k = 0, 1, \ldots, n \quad (8)$$

In the simulations, we will keep the values of C_x, and R_x fixed at $C_x = 1.0\mu F$, $R_x = 1.0K\Omega$. A Pspice subcircuit implementation of this nonlinear capacitor is

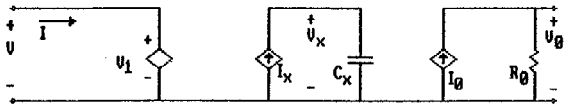

Fig. 4. Circuit realization for the nonlinear capacitor.

given in Fig. 5. Note that in Fig. 5, a large resistor, R_{inf}, is included between the nodes 30 and 90 to provide a DC path required by Pspice.

As we stated earlier, for the purpose of numerical simulations, it is almost always easier to work with the nondimensional (and normalized) parameters. However, for the purpose of Pspice simulations, it is more meaningful to use realistic element values. Below, we give an example of how to obtain a set of realistic element values from a given set of nondimensional parameter values. For that purpose, using (4), and (5), let us express the actual parameters in terms of the nondimensional parameters

$$\begin{aligned} G &= \frac{I_0}{\eta V_0} = \frac{\alpha q_0 \omega_0}{V_0} \\ C &= \frac{G}{\gamma \omega_0} \\ L &= \frac{V_0}{I_0 \omega_0 \beta} \\ a_1 &= \frac{a V_0}{q_0} \\ a_3 &= \frac{b V_0}{q_0^3} \\ G_0 &= (m_0 - 1)G \\ G_1 &= (m_1 - 1)G \\ B_p &= \varepsilon V_0 \end{aligned} \quad (9)$$

It is clear from (9) that the number of unknowns is greater than the number of equations. Although we have $(\varepsilon, B_p) = (1, 1)$, we are still left with two degrees of freedom, which means the solution set is not unique. Note that the choice of ω_0 is a very crucial one since it corresponds to the fundamental frequency of oscillation. For that reason, one must choose ω_0 well within the range where the operation of op amps can still be considered frequency-independent. For example, let us choose $(R, \omega_0) = (1K, 10Kr/s)$. Then, using $(\varepsilon, B_p, \eta, \gamma, \alpha, \beta, a) = (1, 1, 1, 1, 9, 100/7, 1)$

```
Subcircuit for charge controlled nonlinear cap, b = −0.01
.SUBCKT NONLINC 10 90
* a = 1.0, b = −0.01
Vdead 10 20 DC 0
E1 20 90 40 90 1.0
F1 90 30 Vdead 1.0
Rinf 30 90 100MEG
Cx 30 90 1.0u
Rx 40 90 1.0K
G1 90 40 poly(1) 30 90 0 0.09 0 -7.29
.ENDS NONLINC
```

Fig. 5. A Pspice subcircuit implementation of the nonlinear capacitor.

```
Example input file, Chua NLC, b = −0.01, m0 = .85 m1 = 0.6
*
VCC 111 0 DC 10.0
VEE 0 222 DC 10.0
.param w0 = 10000, Rs = 1000, m0 = −0.85, m1 = 0.6, alfa = 9.0, beta = 14.2, p1 = 8
.param r11 = p1*Rs/(m1 − m0), r22 = Rs/((m1 − m0)/p1 − (m1 − 1))
L 1 0 Rs/(beta*w0)
R 1 2 Rs
C 1 0 1.0/(Rs*w0)
XANC 2 0 NONLINC
*For the subcircuit op amp model AD712 V+ V- VCC VEE Vout
*Please reffer to reference [8]
XA1 2 4 111 222 3 AD712
R1a 2 3 r11
R2a 3 4 r11
R3a 4 0 r11/7.0
XA2 2 6 111 222 5 AD712
R4b 2 5 r22/10.0
R5b 5 6 r22/10.0
R6b 6 0 r22
*Subcircuit for charge controlled nonlinear cap, b = −0.01
.SUBCKT NONLINC 10 90
*
Vdead 10 20 DC 0
E1 20 90 40 90 1.0
F1 90 30 Vdead 1.0
Rinf 30 90 100MEG
Cx 30 90 1.0u
Rx 40 90 1.0K
G1 90 40 poly(1) 30 90 0 0.09 0 -7.29
.ENDS NONLINC
.IC V(2) = 0.1
.TRAN 0.01MS 75.0MS 50.0MS 0.01MS
.probe
.end
```

Fig. 6. An overall Pspice input circuit for $b = -0.01$.

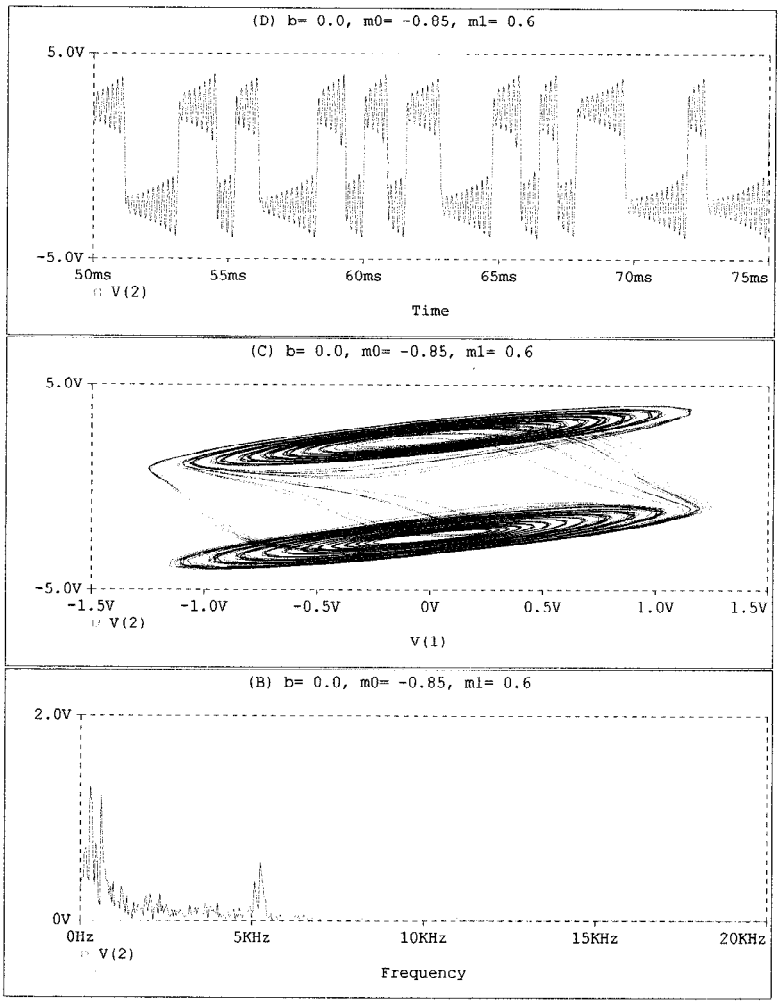

Fig. 7. Pspice simulation results for $(m_0, m_1, b) = (-.85, .6, 0.0)$.

we obtain

$$V_0 = 1.0V, \quad I_0 = 1.0mA, \quad q_0 = 11.11nC$$

$$C = 100nF, \quad L = 7mH$$

$$a_1 = 9 \cdot 10^7 V/C, \quad a_3 = 729 \cdot 10^{21} \cdot bV/C^3 \quad (10)$$

$$G_0 = (m_0 - 1)mS, \quad G_1 = (m_1 - 1)mS$$

Since we have already chosen $(R_x, C_x) = (1.0K, 1.0\mu F)$, we obtain the coefficients for the polynomial dependent source as

$$b_1 = 0.09 \qquad b_3 = -729 \cdot b \qquad (11)$$

An overall Pspice input circuit for $b = -0.01$ is given in Fig. 6.

For the purpose of verifying the bifurcation diagram of Fig. 3 by Pspice simulations, we use a one-dimensional sweep of the (m_0, m_1) parameters for different values of b. By one-dimensional sweep, we mean that we keep m_1 fixed at a value (e.g., $m_1 = 0.6$) so that the line $m_1 = const$ passes through all three regions in Fig. 3. Thus, for each value of b, m_0 is changed such that the points (m_0, m_1) fall both within and outside the chaotic region at hand. In this manner, we obtain nine different simulation results as shown in Figs. 7, 8, 9, 10, 11, 12, 13, 14, 15. In these figures, the top portion is the time behavior of the state variable $v_2(t)$, the middle portion is the $v_1 - v_2$ phase plane, and the bottom portion is the frequency spectrum of $v_2(t)$. By looking at these figures, we see chaotic behavior in

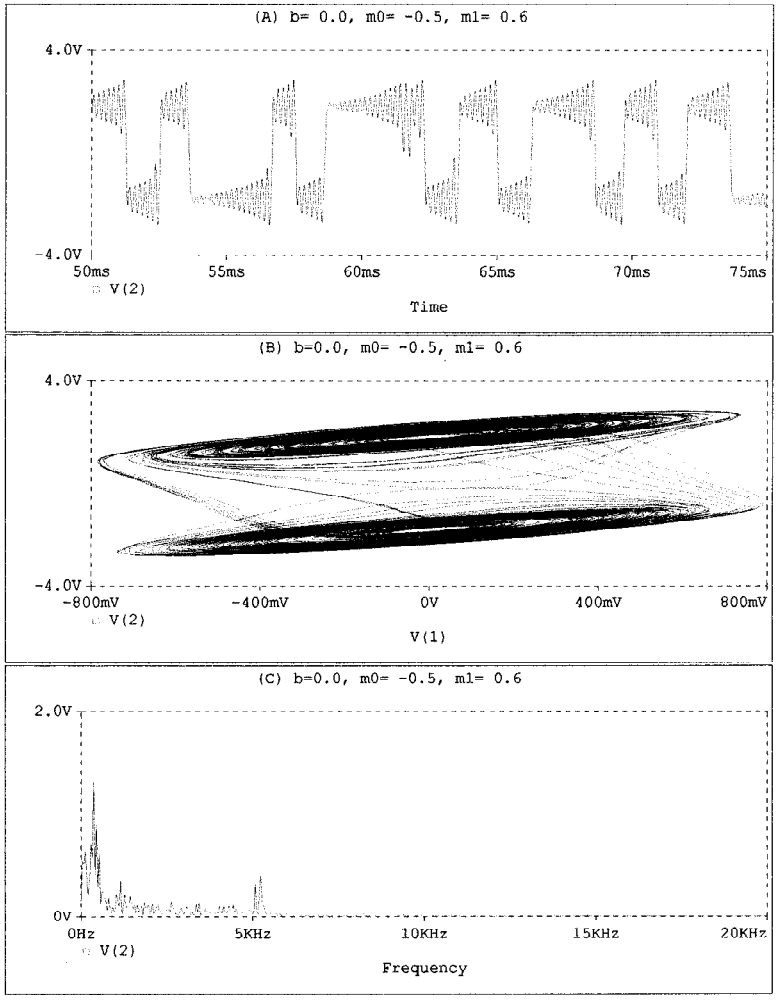

Fig. 8. Pspice simulation results for $(m_0, m_1, b) = (-.5, .6, 0.0)$.

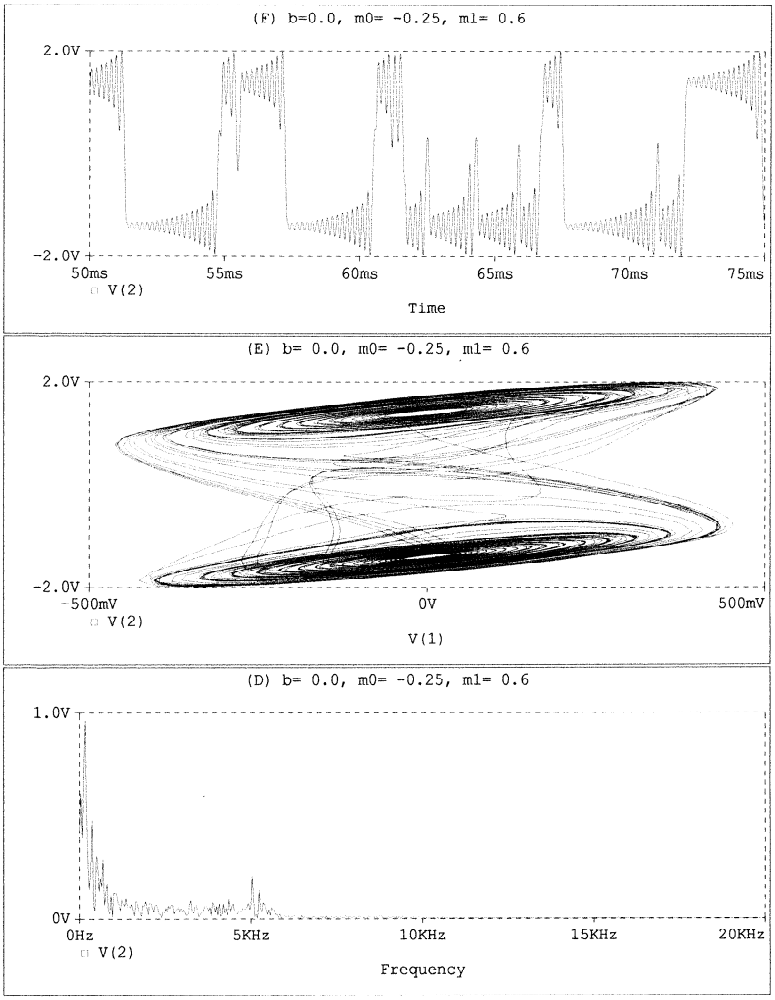

Fig. 9. Pspice simulation results for $(m_0, m_1, b) = (-.25, .6, 0.0)$.

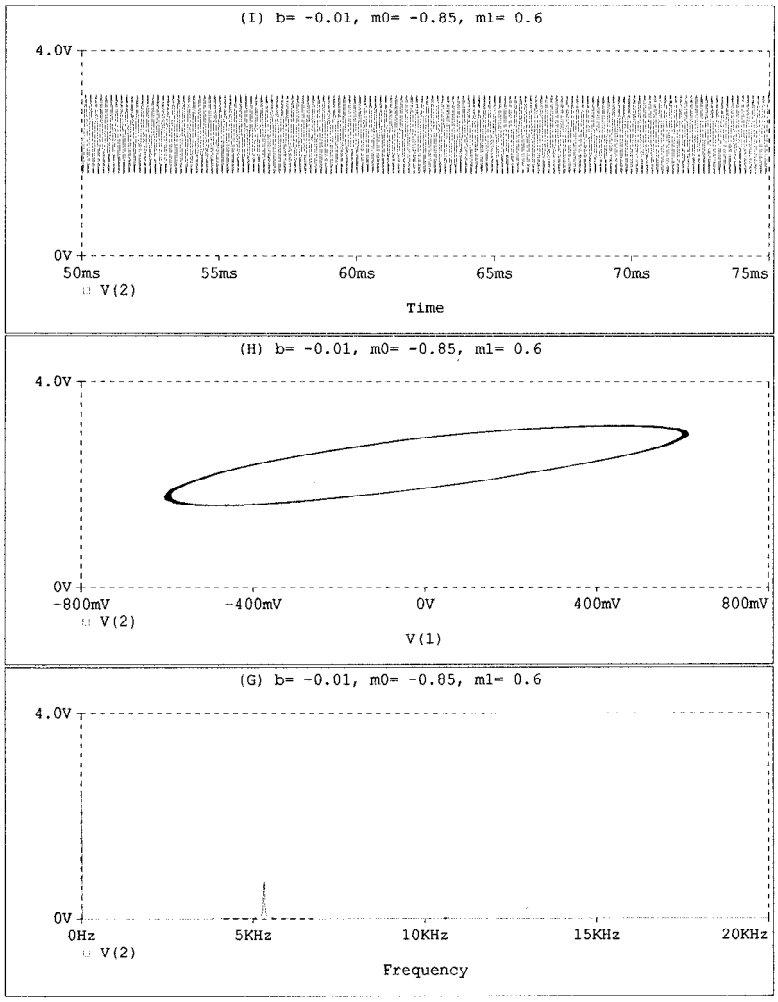

Fig. 10. Pspice simulation results for $(m_0, m_1, b) = (-.85, .6, -.01)$.

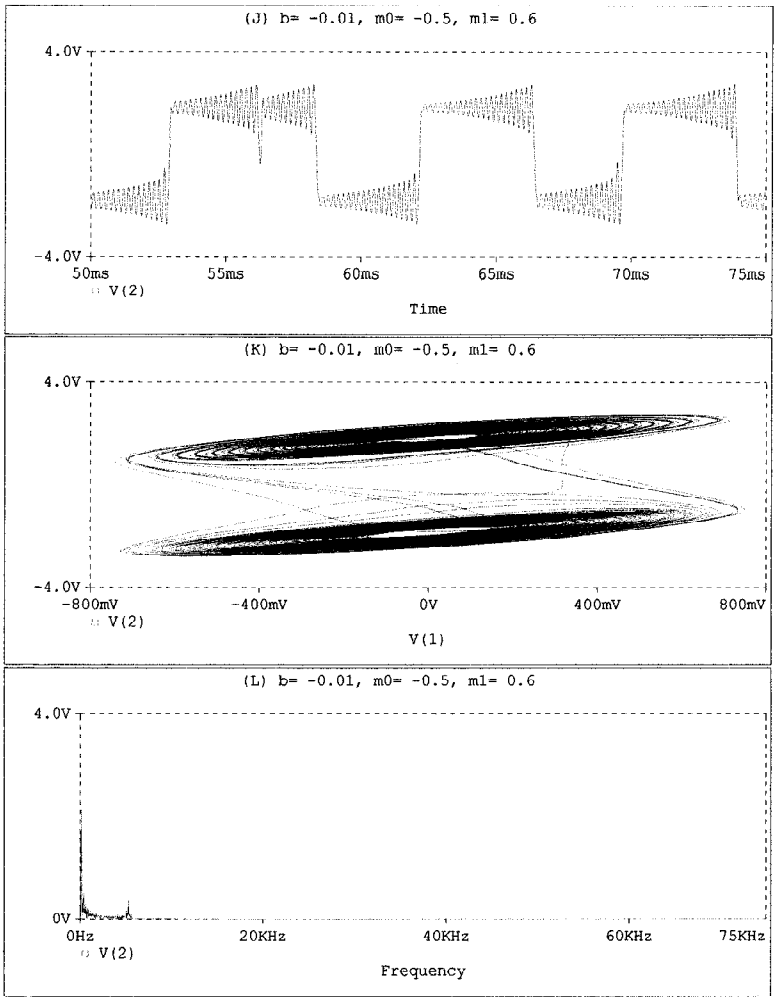

Fig. 11. Pspice simulation results for $(m_0, m_1, b) = (-.5, .6, -.01)$.

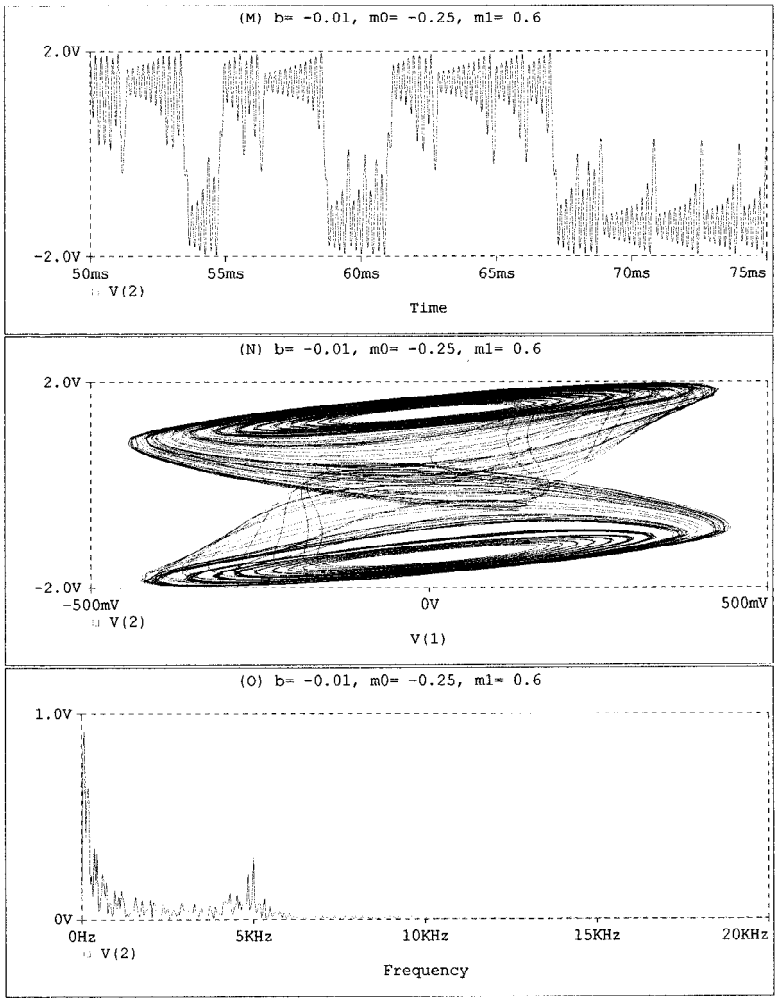

Fig. 12. Pspice simulation results for $(m_0, m_1, b) = (-.25, .6, -.01)$.

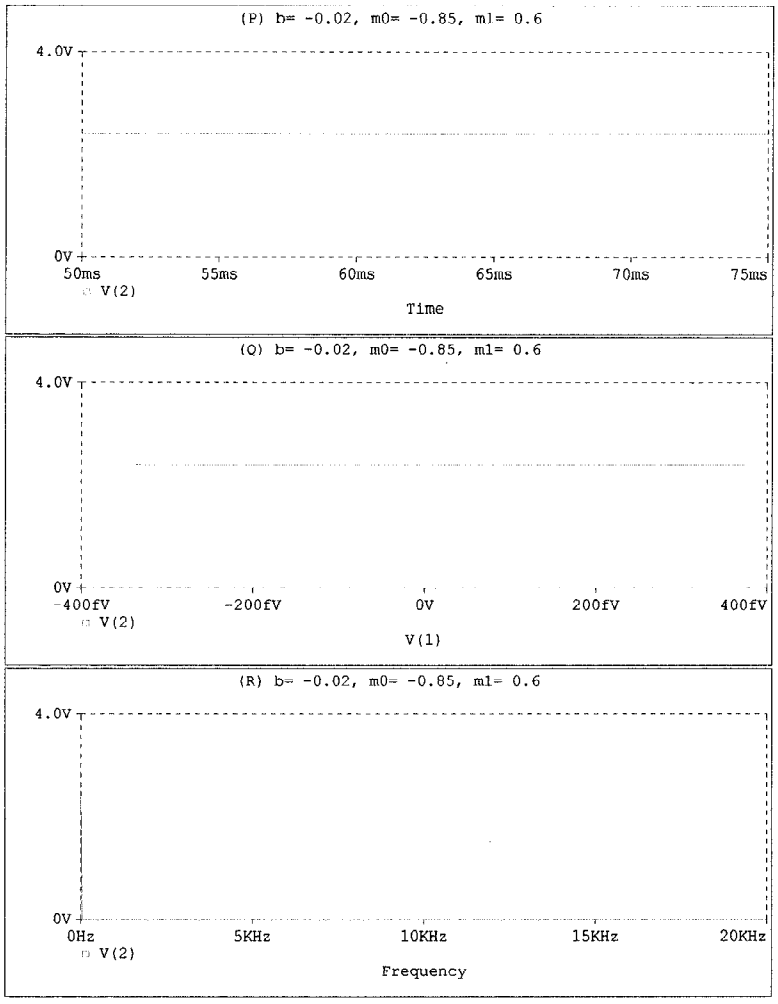

Fig. 13. Pspice simulation results for $(m_0, m_1, b) = (-.85, .6, -.02)$.

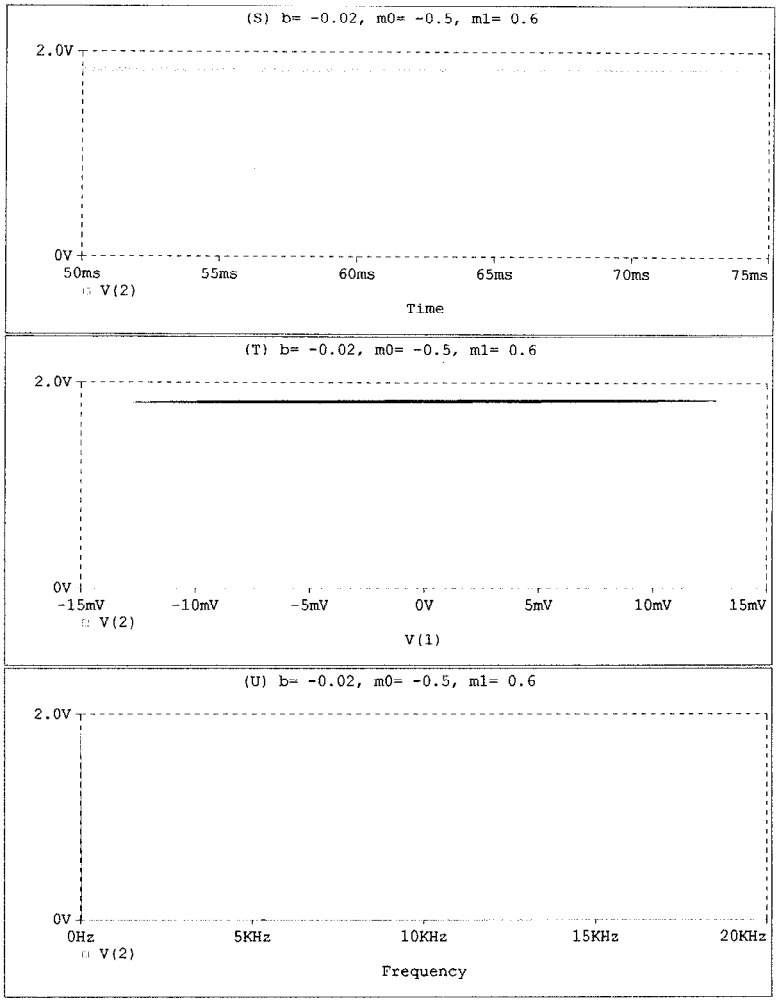

Fig. 14. Pspice simulation results for $(m_0, m_1, b) = (-.5, .6, -.02)$.

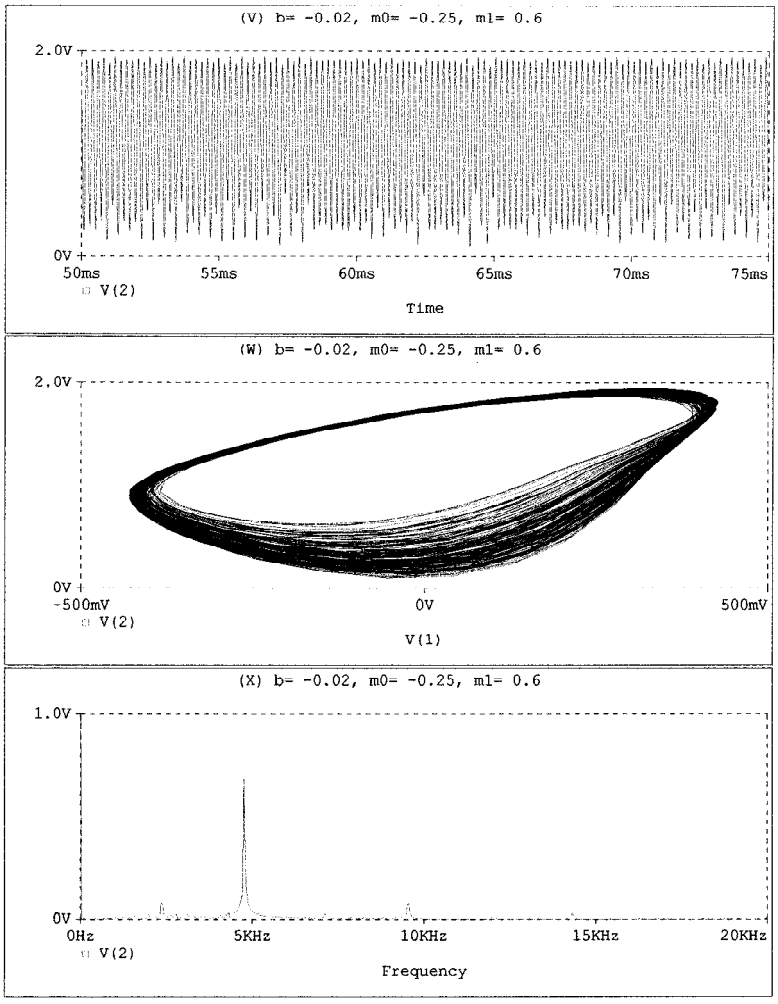

Fig. 15. Pspice simulation results for $(m_0, m_1, b) = (-.25, .6, -.02)$.

Figs. 7, 8, 9, 11, 12, 15 and regular behavior in Figs. 10, 13, 14, which agrees with the bifurcation diagram of Fig. 3.

5. Conclusion

The results of our numerical investigation supported by the Pspice simulations have shown that the interaction of capacitive and resistive nonlinearities can limit the range of the system parameters for chaotic behavior as was indicated in [10]. As a conclusion, we can say that such investigations deserve more attention in terms of experimental and theoretical analysis, and can be useful in the context of controlling and limiting chaos.

Notes

1. A. Oksasoglu is currently on leave from The University of Çukurova, Adana, Turkey.

References

1. T. Matsumoto, "A chaotic attractor from Chua's circuit." *IEEE Trans. Circuits Syst.* CAS-31, pp. 1055–1058, Dec. 1984.
2. G.-Q. Zhong and F. Ayrom, "Experimental confirmation of chaos from Chua's circuit." *Int. J. Circuit Theory Appl.* 13, pp. 93–98, Jan. 1985.
3. L. O. Chua, M. Komuro, and T. Matsumoto, "The double scroll family, Parts I and II." *IEEE Trans. Circuits Syst.* CAS-33, pp. 1073–1118, Nov. 1986.
4. J. M. Cruz and L. O. Chua, "A CMOS IC nonlinear resistor for Chua's circuit." *IEEE Trans. Circuits Syst.* CAS-39, pp. 985–995, 1992.
5. M. P. Kennedy, "Robust op amp realization of Chua's circuit." *Frequenz* 46, pp. 66–80, 1992.
6. Roger Conant, *Engineering Circuit Analysis with Pspice and Probe*. McGraw-Hill: New York, 1993.
7. E. J. Altman, "Normal form analysis of Chua's circuit with application for trajectory recognition." *IEEE Trans. Circuits Syst. 40(10)*, pp. 675–682, 1993.
8. G. Sarafian and B. Z. Kaplan, "A new approach to the modeling of the dynamics of RF VCO's and some of its practical implication." *IEEE Trans. Circuits Syst.* 40(12), pp. 895–901, 1993.
9. G. Sarafian and B. Z. Kaplan, "Is the colpitts oscillator a relative of Chua's circuit." *IEEE Trans. Circuits Syst.* 42(6), pp. 373–376, 1995.
10. D. M. Vavriv and A. Oksasoglu, "Stability of varactor circuits." *Electron. Lett.* 30(6), pp. 462–463, 1994.
11. M. P. Kennedy, "Three steps to chaos—Part II: A Chua's circuit primer." *IEEE Trans. Circuits Syst.* CAS-40, pp. 657–674, 1993.

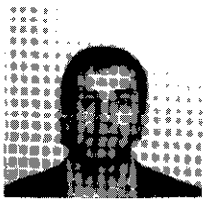

Ali Okşaşoğlu was born in Turkey in 1960. He received the B.S. degree in Electrical Engineering from the Technical University of Istanbul, Turkey in 1983, and the M.S. and Ph.D. degrees in Electrical Engineering from the University of Arizona, Tucson, AZ in 1987 and 1990, respectively. He is currently an associate professor in the Department of Electrical and Electronics Engineering, Çukurova University, Adana, Turkey. His major research interests are linear and nonlinear circuit theory, analog filters, numerical analysis and chaos.

Lawrence P. Huelsman received the Ph.D. degree from the University of California at Berkeley. He is a Life Fellow of the Institute of Electrical and Electronics Engineers. He is currently Professor Emeritus of Electrical and Computer Engineering at the University of Arizona. Dr. Huelsman has written or contributed to twenty books, ten as author, four as coauthor, four as editor, and two as contributing editor. He has written over 100 technical papers. He is a member of of the program committees for the Midwest Symposium on Circuits and Systems and the International Conference on Simulation in Engineering Education. He is Associate Editor for several professional journals, including *Computer Applications in Engineering Education*, *Circuits and Devices Magazine*, and *IEEE Transactions on Education*. He has received the Anderson Prize of the College of Enginering and Mines of the University of Arizona for his contributions to education. He has received the 1995 Society Education Award of the IEEE *Circuits and Systems Society in recognition of his contributions* to circuit theory education.